Philips Res. Repts 22, 267-288, 1967

# EVOLUTIONARY SELECTION, A PRINCIPLE GOVERNING GROWTH ORIENTATION IN VAPOUR-DEPOSITED LAYERS

by A. van der DRIFT

**Abstract**

The preferred orientation of vapour-deposited layers can originate from several stages of the evaporation. It is shown that an increase in the orientation sharpness during the vertical growth points to a process of "evolutionary selection". This process is discussed and visualized. The orientation is calculated as a function of the angle of incidence for a number of typical, most extreme, cases. Special attention is paid to the effect of the surface diffusion on the orientation. Several errors that can easily be made in studying the growing mechanism are discussed.

## 1. Introduction

In a previous paper [11]) a mechanism for which we proposed the name of "evolutionary selection" was suggested to explain the texture *) of a vapour-deposited PbO layer. In the present paper we will consider the evolutionary selection and its theoretical consequences as generally as possible.

Surveys of experiments and attempts made to understand the different causes of orientations have been given by Mayer [1]), Evans and Wilman [2]), Bauer [3]) and Clapp [4]). Other results have been published since [5–11]).

For convenience the geometrical parameters to be used are defined in fig. 1. Two angles of incidence have to be distinguished: $\eta_i$, the angle between the molecular beam and the normal to the crystal face $i$, and $\gamma$, the angle between the molecular beam and the normal to the substrate. Sometimes a special case, referred to as a simplified case to distinguish it from the general case, is assumed in which either the normal to a crystal face or a platelet under consideration, or a needle is lying in the plane formed by the molecular beam and the normal to the substrate.

## 2. Possible causes of textures

The textures can be classified according to the stage of deposition at which they arise: nucleation, horizontal growth of the nuclei and vertical growth of the closed layer. These stages have been observed with the help of electron microscopy [13,14,16,22]), horizontal electrical conduction [5,16]) and material acceptance [15,18]).

*) We use the word texture in the most general sense, not limited to the crystallographic orientation only.

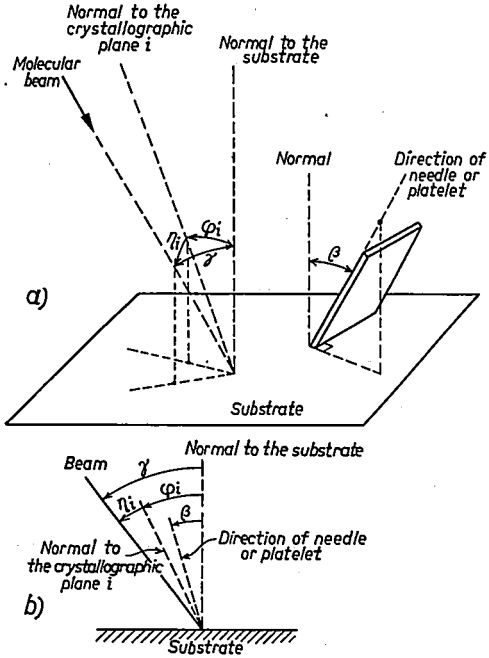


Fig. 1. The significance of the symbols used in the text in three-dimensional cases (*a*) and in two-dimensional approaches (*b*). The arrows point in the positive direction.

The textures can also be divided up according to the number of degrees of freedom lost: three (II-0 in Bayer's [17]) notation), for example, in the typical case of epitaxy and two (I-0), for example, when definite crystal planes tend to be parallel to a smooth substrate. Bauer [17]) does not mention the loss of one degree of freedom, a possibility that can, indeed, easily be overlooked. The case of a crystal plane making a given angle with the substrate is an example of the loss of one degree of freedom. This special orientation is clearly accompanied by a rather weak orientation perpendicular to the substrate, hence characterized by the loss of two degrees of freedom (fig. 2). Often attention will be paid only to the latter orientation. Things like this may have been Reimer and Freking's reasons for saying that the right information can be obtained by examining one material thoroughly rather than measuring too little of too many materials [10]).

By combination of several proposed classifications [10,19]) the following causes of textures can be distinguished:

(a) Initial preferred orientation of the very nuclei.

(a.1) Epitaxy on a monocrystalline substrate that imposes its regularity upon the deposit. There is no change of the orientation sharpness during the horizontal growth of the nuclei and at most a slight decrease during the vertical growth. The orientation is independent of the angle of incidence.

(a.2) Epitaxy on a polycrystalline substrate.

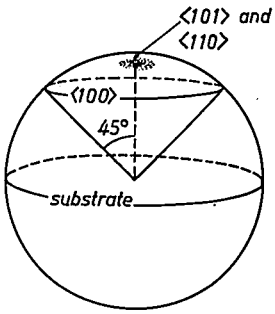


Fig. 2. The ⟨100⟩-direction of a cubic crystal makes angles of 45° with the normal to the substrate: an example of the loss of one degree of freedom. A circle on the unit sphere represents these directions. The surprising consequence of this orientation is another one: a weak orientation of the ⟨101⟩- and the ⟨110⟩-direction perpendicular to the substrate, hence characterized by the loss of two degrees of freedom. Often only the latter orientation will be observed.

(a.3) There is a preference for a certain set of crystal planes to be formed parallel to the amorphous smooth substrate giving rise to the loss of two degrees of freedom independent of the angle of incidence $\gamma$. According to most authors these planes are assumed to be the dense ones. The orientation sharpness remains constant during the horizontal growth of the nuclei, despite re-orientations of the nuclei when touching one another [13]) and can decrease during the stage of vertical growth.

(a.4) The same case (a.3), but on a rough substrate. Evans and Wilman [2]) show how the preferred orientation can depend on the angle of incidence $\gamma$ and the roughness of the substrate. In this case an increase of the orientation sharpness in the stage of horizontal growth of the nuclei and a decrease in the stage of vertical growth may occur.

(b) Growth orientation. Even starting from random nuclei, a preferred orientation develops.

(b.1) The lateral growth rate of the nuclei depends on their orientations. A possible mechanism showing an angle-of-incidence effect has already been suggested by Burgers and Dippel [20]). The orientation sharpness decreases during the stage of vertical growth.

(b.2) The vertical growth rates of the crystals depend on their orientations. Selection takes place because of the differences of the growth rates. This process, for which we proposed the name of evolutionary selection [11]), is the cause of an important difference from all previous cases: the orientation sharpness increases during the vertical growth. This case, which is often encountered [7,8,9,11]), will be more fully discussed in the following sections. The loss of one, two or three degrees of freedom and all kinds of angle-of-incidence effects can be found.

(c) Recrystallization orientation. The orientations change because of interaction between, at least partly, grown-out crystals. Only existing orien-

tations formed as described in the previous cases can become sharper. Independent new orientations are not formed, at best a delayed accommodation to the substrate surface is possible. Reimer and Freking's [10]) supposition that recrystallization is the cause of textures in a gold layer probably deals with a temperature-dependent recrystallization of nuclei belonging to case (a.3).

Of course it is possible that more than one of the causes mentioned above can contribute to a texture.

### 3. The principle of evolutionary selection

The expression evolutionary selection, already used several times, has to be taken in the general sense; evolution of a population can occur only when there is a selection because of a property of the individuals determining the probability of survival. In the case of vapour-deposited layers it appears to be necessary to consider as such a property the vertical growth rate of the individual crystals, the rate at which the highest point of the crystal rises. The bigger the vertical growth rate, the greater the probability of survival. Hence only a few favoured orientations (with nearly maximum vertical growth rate) will be left over in the final instance, all other orientations gradually dying out. This is shown in fig. 3

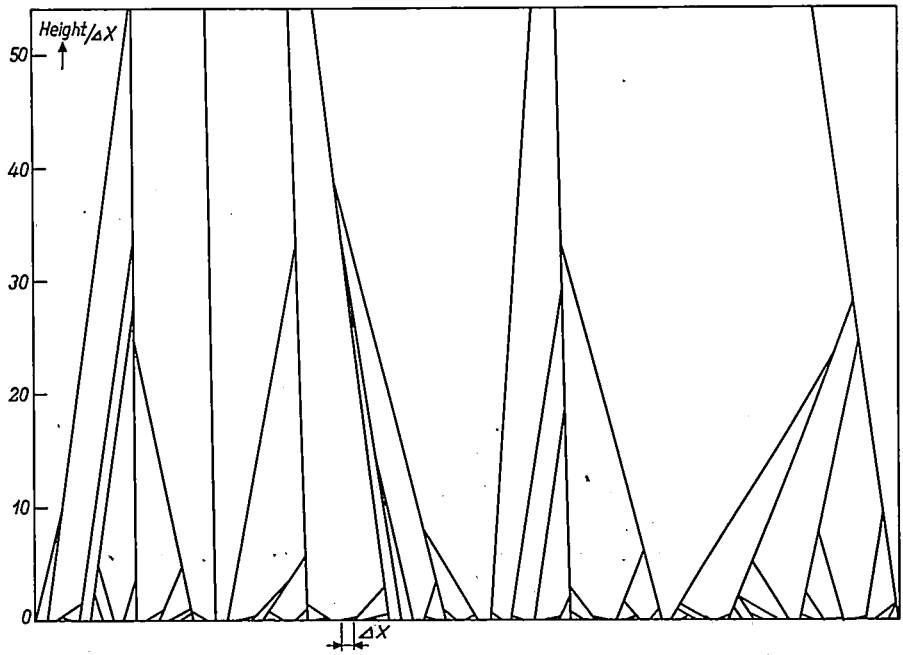


Fig. 3. The evolutionary selection during growth starting from randomly orientated equidistant nuclei on a one-dimensional substrate (bottom line) in a two-dimensional space, is shown. The assumption is that the vertical component of the growth rate is larger at steeper orientations of the crystal. The height above the substrate is expressed in the unit $\Delta x$, the distance between two nuclei.

for the case of a two-dimensional space (on the page) in which one-dimensional crystals grow on a one-dimensional substrate. The assumption is that the vertical growth rate is bigger the steeper the orientation. If two crystals meet, the less steep one ends in the flank of the steeper one: the survival of the fastest. In a real layer things are somewhat more complicated. Nevertheless the same principle obviously applies.

Due to the simplicity of the selection rule, it is often quite possible to calculate the final preferred orientation by determining the orientation with maximum vertical growth rate. This can be done by adding up the contributions to it from all crystal faces. Each contribution is proportional to the number of impinging molecules per unit area, the acceptance $A$ of the impinging molecules and a factor depending on geometry and orientation of the crystal.

Molecules deposited between the selected crystals may form random nuclei again. These nuclei can grow according to the same selection rules, however, with the disadvantage of growth in the depth. At most they will make the orientation sharpness weaker.

## 4. Characteristics of the deposited material controlling the texture

Let us assume that only the evolutionary selection of sec. 3 plays a part in the formation of a texture which, hence, develops even starting from random nuclei. It is then easy to understand that the final texture is fully determined when the way in which the crystal grows in every possible orientation under the conditions of the deposition is known. To this end it would be sufficient to know of each crystal face: the probability $A$ for landing molecules to be adsorbed as a function of the angle of incidence $\eta$, the thermodynamic probability of adsorbed molecules becoming part of the crystal and all data pertinent to the surface diffusion. These characteristics are independent of one another. Unfortunately very little is known about them. A characteristic far easier to measure is the shape of the crystals as orientated under the conditions of the deposition. This crystal shape, rather a result than a cause, can replace some other material characteristics. As we shall see later, it is often impossible to recognize any crystal shape in the layers, either in the case of high density of that layer, or in the case of a growth direction independent of the crystal orientation. In those cases there is still another readily accessible characteristic of the material: the shape of a single crystal as formed at isotropic supply.

In addition to the crystal shape, assumptions regarding the surface diffusion have to be made. We shall consider the extreme cases of no surface diffusion and infinite surface diffusion. The latter will be considered separately in the cases of diffusion even along the substrate, diffusion restricted to the individual crystals and diffusion restricted to the individual crystal faces.

Finally, assumptions regarding the function $A = f(\eta)$ have to be made. Little is known about the acceptance $A$, defined as the part of impinging

molecules that remains adsorbed even after a long time (the latter addition to distinguish it from the condensation coefficient, which applies only after a very short time).

Mayer [1]) and Ehrlich [23]) suppose a condensation coefficient of unity but, like Langmuir [12]), also assume a certain probability of reevaporation after some time, possibly after a shift along the crystal surface. In these cases the acceptance is probably not dependent on the angle of incidence $\eta$. This is not the case either, according to Johnson [15]) who assumes the acceptance $A$ of CdS in the stage of vertical growth (sec. 2) to be unity.

Goodman [27]) shows the possibility of a condensation coefficient considerably smaller than unity; $\eta$ dependence of $A$ then has to be considered. This dependence has been studied by several authors for the impact of ions on a crystal. In the high-energy case considered by Snoek and Kistenmakers [24]) and Brunnée [25]) it appears to be a matter of two-particle interactions giving rise to more reflection at more glancing incidence. Weijsenfeld [26]) considers the impact of low-energy ions. Multi-particle interaction can give rise to somewhat less reflection at more glancing incidence. Vapour depositions have some relation to ion-impact phenomena at lower energy (much more than with neutron impact which leads Bauer [17]) to suggest a rather complicated relation) but a choice as to the dependence of the acceptance from $\eta$ cannot be made. For convenience in this paper three representative cases will be distinguished: $A$ is independent of $\eta$ and $A$ is proportional to $\cos\eta$ or $\sin\eta$, to represent steadily decreasing and increasing functions, respectively.

## 5. Evaluation of some extreme cases

The following subsections deal with the orientation and its dependence on $\gamma$ for several, most extreme, assumptions about the surface diffusion.

### 5.1. *Infinite surface diffusion even along the substrate*

The possibility of transport along the substrate surface has often been proved, e.g. by Volmer [21]) and Van der Waterbeemd [22]).

The molecules, after having been accepted, are fully redistributed. There will therefore be no memory of the angles of incidence $\gamma$ or $\eta$. Only the thermodynamically most favourable crystal faces will grow. Thus, strictly speaking, we get three-, two- or one-dimensional crystals. For simplicity we shall consider the latter two to be platelets and needles, respectively. In the case considered in this subsection, all crystals grow equally quickly, therefore the crystals with the direction of fastest growth nearly perpendicular to the substrate are in a favoured position in relation to other crystals and will survive. The orientation obtained is characterized by the loss of two degrees of freedom.

Which crystallographic direction is the one of fastest growth? When the surface diffusion is infinite, crystals in a deposited layer and free-growing crystals

expand in the very same way. In the latter crystals the direction of fastest growth is obviously the direction from the centre towards the remotest point of that crystal (see fig. 5).

Platelets and needles will therefore tend to stand upright. This is in accordance with an experiment of Volmer [29]), also described by Mayer [1]), involving the

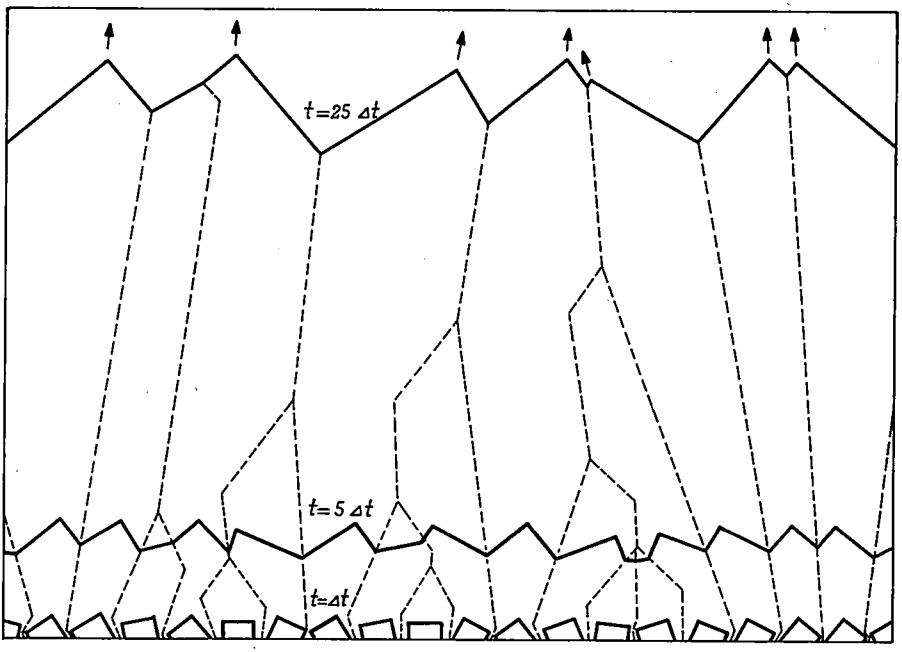


Fig. 4*a*. Starting from random-orientated equidistant (10)-bounded "cubic" crystals in a two-dimensional space and assuming infinite surface diffusion even along the substrate, the inter-crystal boundaries (dashed lines) as well as the crystal front at different times (at $t = \Delta t$, $t = 5\,\Delta t$ and $t = 25\,\Delta t$ in which $\Delta t$ is the shortest time required for two neighbouring nuclei to meet one another) are constructed. It is shown how the evolutionary selection leaves the crystals with their ⟨11⟩-direction (arrows) nearly perpendicular to the substrate.

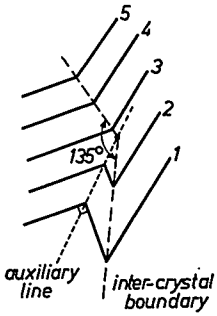


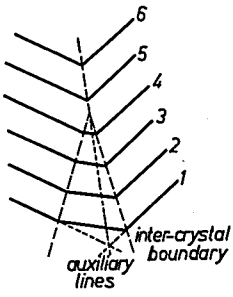


Fig. 4*b*. The inter-crystal boundaries (dashed lines) change their direction at definite points. The construction of the two possible cases is shown. The numbers indicate some subsequent crystal fronts.

growth of Hg crystals, made to prove surface diffusion; Volmer's Hg platelets are indeed extremely thin and stand perpendicular to the substrate.

Whereas platelets and needles form porous layers, three-dimensional crystals will fill the space available and form dense layers. In the case of a (10-)bounded two-dimensional "cubic" crystal in a two-dimensional space, evolutionary selection proceeds in a way as shown in fig. 4*a*, where $\Delta t$ is the shortest time required for neighbouring nuclei to meet one another. The construction is explained in fig. 4*b*. Apparently the ⟨11⟩-direction becomes more and more perpendicular to the substrate.

In fig. 5 the direction of fastest growth is shown for a number of arbitrarily chosen crystals. The deposited layer will have this direction nearly perpendicular to the substrate. There is a surprising agreement with some orientations as determined by Bauer [28]) on the assumption of all-side supply. Although isotropic supply and infinite surface diffusion are indeed indistinguishable in their results, we do not agree with Bauer's explanation.

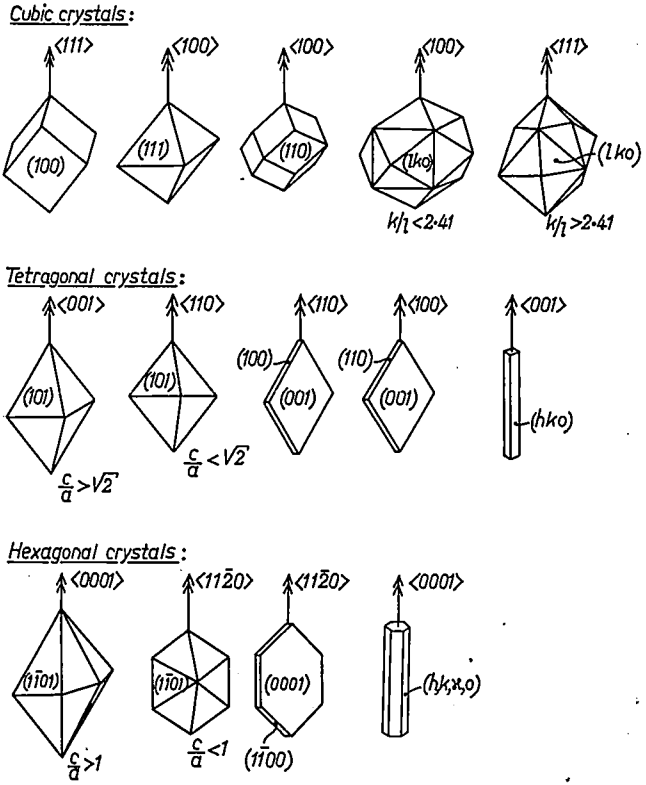


Fig. 5. The direction of fastest growth (double arrows) of a number of free-growing single crystals is constructed. Assuming infinite surface diffusion even along the substrate, crystals with this direction nearly perpendicular to the substrate will gradually determine the preferred orientation of a growing layer.

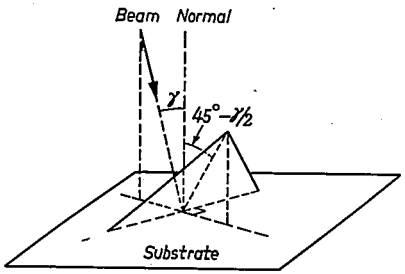


Fig. 6. Preferred orientation of a platelet with infinite surface diffusion but no transport along the substrate and with $A$ independent of $\eta$.

5.2. *Infinite surface diffusion, but restricted to the individual crystals*

Each crystal collects its own material. In the simplified case (sec. 1) and assuming that nearly all the material is provided by the slowest growing and hence most extended planes, the total supply to each crystal is proportional to $\sin(\gamma-\beta)$, regardless of the exact form of the platelet or the needle (see fig. 1 for the meaning of $\beta$). The vertical growth is proportional to $\sin(\gamma-\beta)\cos\gamma$. Calculation leads to the surprising result (fig. 6) that the fastest vertical growth (and hence the preferred orientation) occurs at

$$\beta = \tfrac{1}{2}\gamma - 45°.$$

When the acceptance of the extended plane $a$ of a platelet, $A_a$, is proportional to $\cos\eta_a$, we calculate that the preferred orientation is found when $\beta$ is a solution to

$$\tan(\gamma-\beta)\tan(-\beta) = 2.$$

If, in an otherwise comparable case, $A_a$ is proportional to $\sin\eta_a$, $\beta$ will be a solution to

$$\tan 2(\gamma-\beta)\tan(-\beta) = 2.$$

In fig. 7 these expressions are given graphically.

Unlike platelets and needles, three-dimensional crystals will grow in all directions, thus forming dense layers. As a consequence of the infinite surface diffusion, the crystals in this layer will be bounded by crystallographically equivalent planes. The most favourable orientation of the crystals can be calculated. For example, a (100)-bounded cubic crystal will, at $\gamma = 0$, have its $\langle 111\rangle$-direction preferentially perpendicular to the substrate surface for all three relations considered between $A_t$ and $\eta_t$. Other calculations can be done at will.

We must admit that the combination of parameters chosen in this section, excluding transport even between crystals in close contact, seems rather strange. However, it must be borne in mind that extremes are considered. In practice, intermediate cases will be met with.

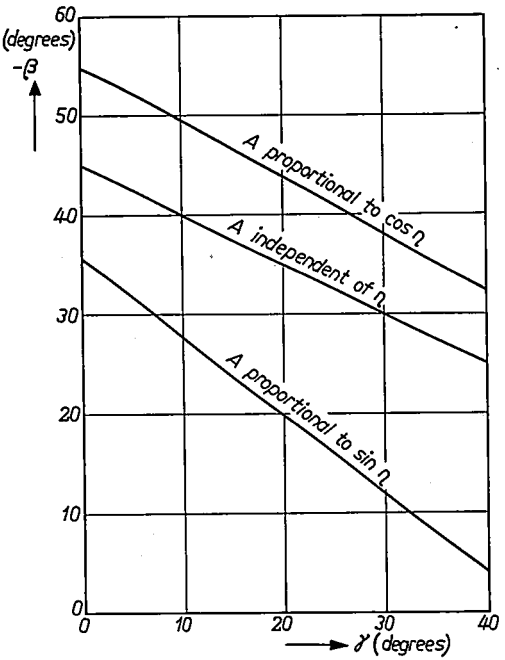


Fig. 7. Relation between $\gamma$ and $\beta$ of preferred-orientated platelets and needles with infinite surface diffusion but no transport along the substrate, for several functions $A = f(\eta)$.

### 5.3. *Infinite surface diffusion, but restricted to the individual crystal faces*

Each crystal face has to collect its own material. The orientations now greatly depend on the assumptions about the acceptance.

#### 5.3.1. The acceptance $A_i$ is independent of the angle of incidence $\eta_i$

In the special case where there are three orthogonal crystal faces for which $A_i$ is independent of $\eta_i$, four different crystal shapes can be distinguished by the following relations between their acceptances:

(a) $A_1 > A_2 > A_3$,
(b) $A_1 = A_2 > A_3$,
(c) $A_1 > A_2 = A_3$,
(d) $A_1 = A_2 = A_3$.

In this case it is possible to calculate the preferred orientation exactly at an arbitrarily chosen value of $\gamma$. This has been done for us by Mr W. P. J. Fontein. The calculations are summarized in appendix A and the calculated preferred orientations are shown in fig. 8. In the simplified case (sec. 1) the occurrence of $\frac{1}{2}\gamma$ in all solutions can easily be understood; the amount of material accepted per unit area of the fastest-growing plane $a$ is then propor-

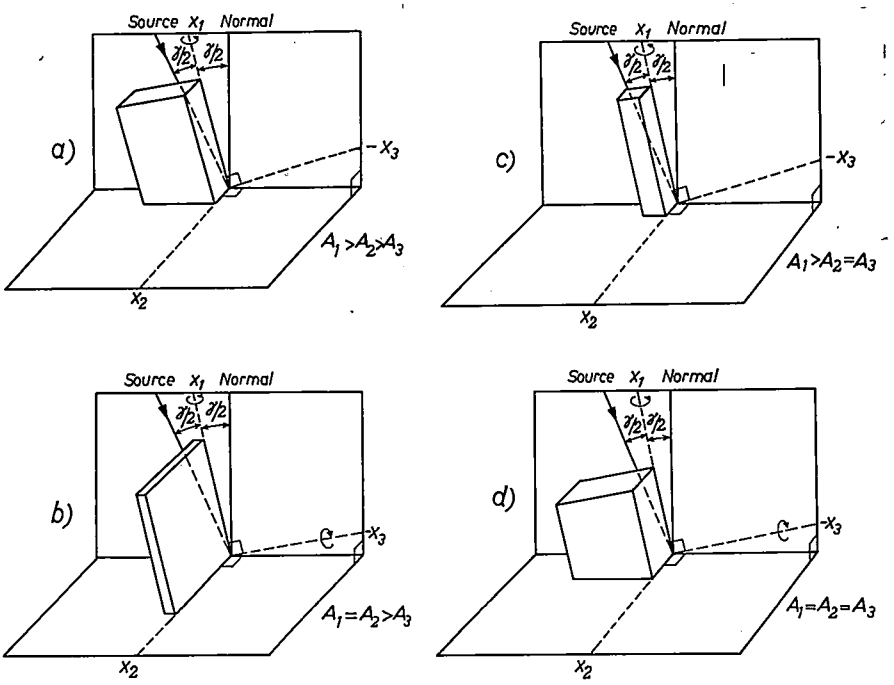


Fig. 8. The calculated preferred orientations of several crystal shapes bounded by three orthogonal sets of planes; $A$ is independent of $\eta$. The surface diffusion is restricted to the individual crystal faces. The crystallographic axes are $x_1$, $x_2$ and $x_3$. The circular arrows indicate the freedom of rotation around the axes.

(*a*) Rhombic crystals bounded by three sets of planes growing at different rates. Two degrees of freedom are lost.
(*b*) Tetragonal crystals bounded by three sets of planes of which one grows more slowly (platelets). One degree of freedom is lost.
(*c*) Tetragonal crystals bounded by three sets of planes of which one grows faster (needles). Two degrees of freedom are lost.
(*d*) Cubic crystals bounded by (100)-planes. One degree of freedom is lost.

tional to $\cos(\gamma - \varphi_a)$, hence the vertical growth rate is proportional to $\cos(\gamma - \varphi_a)\cos\varphi_a$ with a maximum at $\varphi_a = \frac{1}{2}\gamma$.

Platelets and needles with more fast-growing crystal faces can change their crystal shape as a consequence of different growth rates of crystallographically equivalent planes, as is obvious from the example shown in fig. 9. This makes the calculation of the most favourable orientation, even at oblique incidence of the molecules, easier. It may clearly be seen that the perpendicular crystal of fig. 9 is the most favourable one.

### 5.3.2. The acceptance $A_i$ is proportional to $\cos\eta_i$

The contribution of the crystal face $i$ to the vertical component of the growth rate of a crystal is proportional to $\cos^2\eta_i \cos\varphi_i$ or, in the simplified case (sec. 1), to $\cos^2(\gamma - \varphi_i)\cos\varphi_i$. It can be shown that in that case it is suffi-

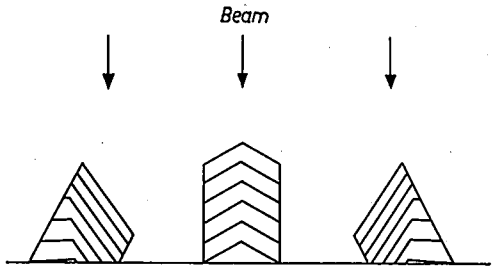


Fig. 9. Different growth rates of crystallographically equivalent planes can cause some crystal faces to disappear, giving crystals of simpler shape. At perpendicular incidence of the molecules the most favoured orientation is the middle one of the three crystals.

cient to consider the contribution of the fastest-growing face $a$. This contribution is maximum if

$$\tan \varphi_a = 2 \tan (\gamma - \varphi_a).$$

At small values of $\gamma$ this means $\varphi_a = \frac{2}{3}\gamma$. Compared with the case of sec. 5.3.1 a crystal has an extra tendency to have its face of fastest growth perpendicular to the molecular beam.

The special case of tetragonal platelets with orthogonal crystal faces has been generally treated, in a similar way to that in sec. 5.3.1. The orthogonal coordinate system is formed by the crystal faces (see fig. 10*b*). The vectors $V_n(\varepsilon_n,\delta_n)$ and $V_s(\varepsilon_s,\delta_s)$, respectively, point in the direction of the normal to the substrate and the direction from which the molecular beam comes; $\gamma$ is the given angle of incidence. With the help of a computer the vertical growth rates are calculated for a large number of admitted values of $V_n$ and $V_s$, and for a large number of different orientations. The orientations of the highest growth rates are selected. In fig. 10*a* these orientations are plotted in the case where $\gamma = 30$ degrees. The results lead to the following conclusions: the maximum growth rate is found at about $\varphi_a = 20$ degrees ($a$ is one of the fastest-growing planes) and a nearly free rotation around this preferred direction occurs. This means, for example, that the alternatives in fig. 11 are about equally probable. Similar calculations have been carried out on the computer for other values of $\gamma$, with the rotational symmetry always shown. Table I gives the values of $\varphi_{a0}$, $\varphi_a$ at maximum vertical growth rate, calculated for several values of $\gamma$.

TABLE I

| $\gamma$ (degrees) | 0 | 10 | 20 | 30 |
|---|---|---|---|---|
| $\varphi_{a0}$ (degrees) | 0 | 7 | 13 | 20 |

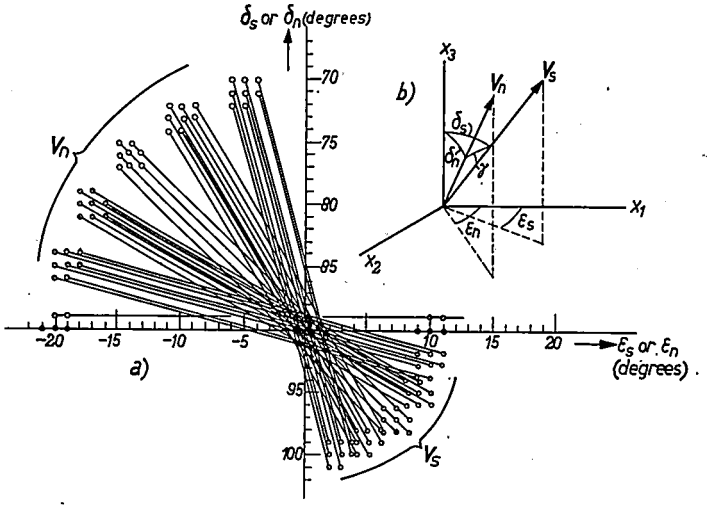


Fig. 10. (*a*) The vertical growth rates at $\gamma = 30°$ are computed from a great number of randomly orientated tetragonal rectangular platelets for which $A_t$ is proportional to $\cos \eta_t$. The orientations with rates differing no more than 0·1 % from the maximum rate have been plotted. The lines connect the two vectors belonging together (as a consequence of crystal symmetry all orientations obtained by reflection at the $\delta$- and $\varepsilon$-axes of this plot are equally probable although they have not been drawn). Conclusions from this figure are drawn in the text.
(*b*) The significance of the coordinates; $\mathbf{V}_n$ is the unit vector representing the direction of the normal to the substrate; the unit vector $\mathbf{V}_s$ is the direction to the vapour source; $\delta$ and $\varepsilon$ are polar coordinates relative to the orthogonal system with three crystal directions $x_1$, $x_2$ and $x_3$ as its axes.

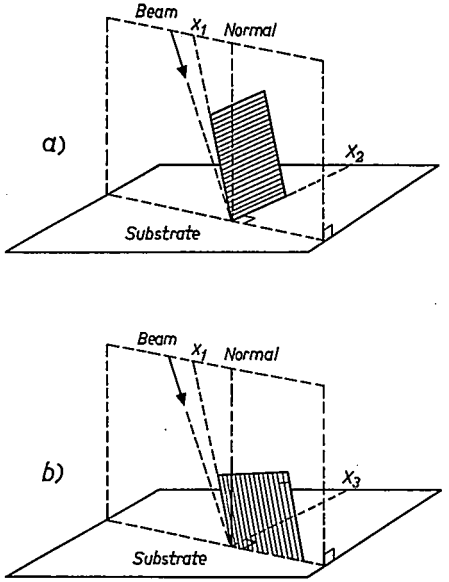


Fig. 11. Two equally probable orientations of the many shown in fig. 10. The simple principle of evolution does not distinguish between them.
(*a*) $\varepsilon_n = \varepsilon_d = 0$, $\delta_n = 70°$, $\delta_s = 100°$.
(*b*) $\delta_n = \delta_s = 90°$, $\varepsilon_n = -20°$, $\varepsilon_s = 10°$.

Our approach in the simplified case was, apparently, fairly accurate in predicting $\varphi_{a0}$ to be about $\frac{2}{3}\gamma$. It remains true even where $\gamma$ ranges to 30 degrees.

### 5.3.3. The acceptance $A_t$ is proportional to $\sin \eta_t$

Again we limit the calculations to a rectangular crystal in the simplified case (sec. 1); $\eta$ of the fastest-growing plane then equals $\beta$. Ignoring the contribution of the slowest-growing plane to the vertical growth rate, we find that $\beta$ must be the solution to

$$\tan 2(\gamma - \beta) \tan(-\beta) = 2.$$

### 5.4. *There is no surface diffusion at all*

Every accepted molecule sticks to the place where it lands. The typical crystal shape is lost. There can only be growth in the direction of the beam. Some scattering of the molecules must be assumed, in fact, since otherwise the crystals would be one-dimensional.

Crystals bounded by crystallographically equivalent planes will also gradually form dense layers of randomly orientated columns when $A$ is independent of $\eta$ (fig. 12). When $A$ is $\eta$-dependent some columns grow faster then others. A preferred orientation will gradually develop as a consequence of extra side-growth.

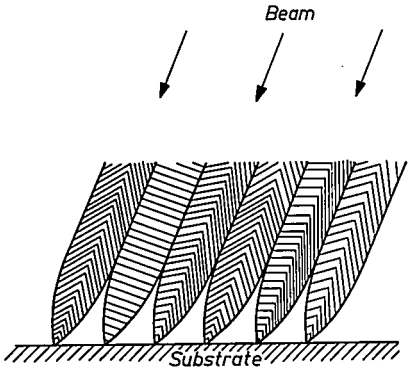


Fig. 12. Growth of crystals bounded by crystallographically equivalent planes without any surface diffusion and $A$ independent of $\eta$. There is no selection of orientations.

Crystallographically different crystal faces will generally obtain a different amount of material as a result of different values of $A$. This causes the fastest-growing faces to disappear as is shown in fig. 13. Crystal edges cannot exist in the final stage of deposition. A very slow growth of the layer is to be expected.

### 5.5. *The surface diffusion has a finite value*

Molecules accepted by one crystal face have a chance of migrating to other faces depending on the point of impingement. Of the many possible assumptions

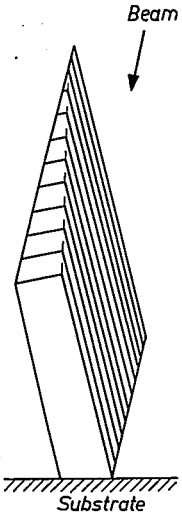


Fig. 13. Cross-sections at several stages of the growth of a crystal with different boundary planes without any surface diffusion, showing the disappearance of the plane with the greater acceptance.

we have selected the following (in the calculation given in greater detail in appendix B):

(a) the crystal is a rectangular platelet with one edge parallel to the substrate (perpendicular to the paper in fig. 14);

(b) on face *a* (fig. 14) the accepted molecules at first behave as a fluid-like material with a probability of solidification proportional to the amount of fluid-like material per unit area;

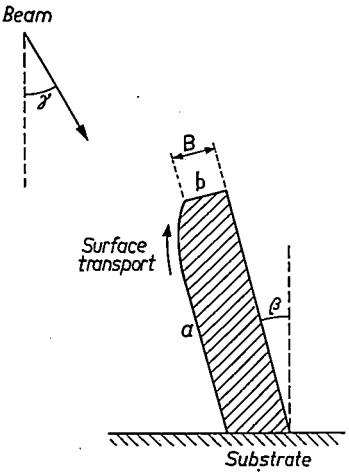


Fig. 14. Model, used in the calculations, of a case of limited surface transport along one crystal face. Some symbols used in the calculation are indicated.

(c) transport of fluid-like material around the edges is not restricted;
(d) face $b$ has an infinite surface diffusion and a high solidification rate;
(e) the acceptances are independent of the angle of incidence $\eta$.

With these assumptions the orientation $\beta$ of crystals having maximum vertical growth rate is obtained from

$$\tan(\gamma - 2\beta) = P,$$

with

$$P = \frac{A_a}{BA_b}\left(\frac{D}{K}\right)^{1/2},$$

where $A_a$ and $A_b$ are the acceptances of $a$ and $b$, respectively, $D$ is the diffusion coefficient of the fluid-like material and $K$ is a constant. The meaning of $B$ is shown in fig. 14. The plots in fig. 15 of the relation between $\gamma$ and $\beta$ for several values of $P$ show the important fact that, in very many cases, either of the approaches $P = 0$ and $P = \infty$ may be used each being a special case already considered in this paper. If $P = 0$, the contribution of plane $a$ to the growth of plane $b$ can be ignored; we are dealing with the simplified case as described in sec. 5.3.1 where we calculated $\beta = \frac{1}{2}\gamma$ for platelets (remember that $\varphi_a$ used in sec. 5.3.1 refers to the fastest-growing plane, so that $\varphi_a = \beta$). If $P = \infty$,

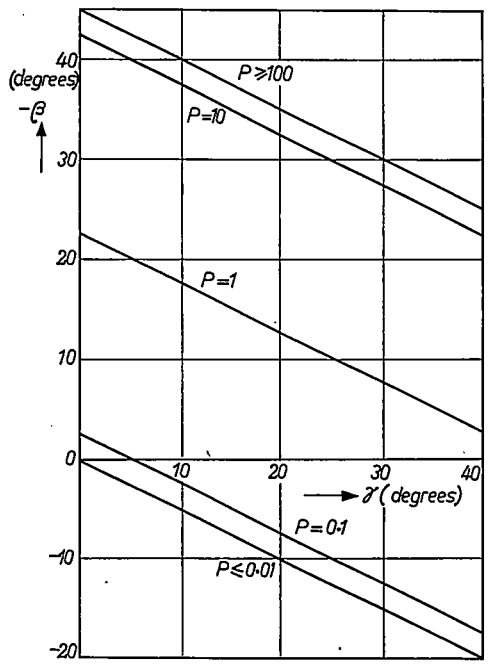


Fig. 15. Relations between $\beta$ and $\gamma$ at several values of $P$ as calculated in appendix B in two-dimensional approach; $P$ is proportional to the root of the surface-diffusion coefficient $D$.

the total supply of material is redistributed; we are dealing with the case as described in sec. 5.2, where we calculated $\beta = \frac{1}{2}\gamma - 45°$ for platelets.

From the considerations in this section it appears to be useful to pay attention to extreme cases in order to obtain information on the intermediate ones.

## 6. Conclusions

An increase in the orientation sharpness during the vertical growth of the layer is a certain indication that we are dealing with a process of evolutionary selection of favourable orientations. The crystals with the highest component of the growth rate perpendicular to the substrate are selected. The "survival of the fastest" is the ruling principle.

The vertical growth rate can be written as a function of the crystal orientation and the angle of incidence on the substrate. In a number of extreme cases it appears to be possible to calculate the preferred orientation and the effect of the angle of incidence on it. Undoubtedly simple considerations based on the principle of evolutionary selection can contribute to a great extent to the understanding of many experimentally found textures.

Three different types of textures can be distinguished: one, two or three degrees of freedom can be lost. It is shown how the first type (loss of one degree) can easily be considered as the second type (loss of two degrees). Errors can also be made in the case of crystal orientation without crystallographic orientation. These two examples show the necessity of a variety of measurements when it is an understanding of the mechanism of growth which is desired; at least electron microscopy as well as several X-ray methods will generally have to be used.

## Appendix A

*The calculation of the preferred orientation as a function of $\gamma$ in the special case of sec.* 5.3.1

Assumptions:

(a) the crystal has as its faces three orthogonal pairs of planes;
(b) the acceptance is independent of the angle at which the molecular beam impinges on the crystal face;
(c) the surface diffusion is restricted to the individual faces.

The orientation of the crystal at maximum growth rate in the direction of the normal to the substrate is to be calculated. To do this the orthogonal coordinate system as formed by the crystal faces is chosen, $\mathbf{x}_1$ is the unit vector along the $\mathbf{x}_i$-axis. The index $i$ is taken so that $A_1 \geqslant A_2 \geqslant A_3$. The unit vectors $\mathbf{V}_n$ and $\mathbf{V}_s$, respectively, point in the direction of the normal to the substrate and the direction from where the molecular beam comes. The coordinates of $\mathbf{V}_n$ and $\mathbf{V}_s$ are defined in fig. 10*b*.

The vertical component $Y$ of the growth rate consists of three contributions $Y_i$, one from each crystal face:

$$Y = \sum_{i=1}^{3} k_i Y_i, \tag{A.1}$$

$$Y_i = (\mathbf{V}_n \cdot \mathbf{x}_i)(\mathbf{V}_s \cdot \mathbf{x}_i). \tag{A.2}$$

The constant $k_i$ has to be introduced because of the impossibility of a negative contribution to the vertical growth. Hence

$$\begin{aligned} k_i &= A_i \quad \text{for} \quad Y_i \geqslant 0, \\ k_i &= 0 \quad \text{for} \quad Y_i < 0. \end{aligned} \tag{A.3}$$

The constancy of $\gamma$, the angle of incidence on the substrate surface, and thus the angle between $\mathbf{V}_n$ and $\mathbf{V}_s$, means

$$\mathbf{V}_n \cdot \mathbf{V}_s = \cos\gamma. \tag{A.4}$$

With the help of the method of Lagrange (A.1), (A.2) and (A.4), after transforming them in trigonometric equations in $\varepsilon_n$, $\varepsilon_s$, $\delta_n$ and $\delta_s$, we obtain the conditional relative maxima of table II.

TABLE II

| | $Y_{\max}$ | orientations |
|---|---|---|
| $k_1 > k_2 > k_3$ | $k_1 \frac{\cos\gamma + 1}{2} + k_3 \frac{\cos\gamma - 1}{2}$ | $\varepsilon_n = \varepsilon_s = 0$<br>$\delta_n = \delta_s = \pi$<br>$\delta_n - \delta_s = \gamma$ |
| $k_1 = k_2 > k_3$ | $k_1 \frac{\cos\gamma + 1}{2} + k_3 \frac{\cos\gamma - 1}{2}$ | $\varepsilon_n = \varepsilon_s$<br>$\delta_n + \delta_s = \pi$<br>$\delta_n - \delta_s = \gamma$ |
| $k_1 > k_2 = k_3$ | $k_1 \frac{\cos\gamma + 1}{2} + k_3 \frac{\cos\gamma - 1}{2}$ | $\varepsilon_n = -\varepsilon_s$<br>$\delta_n + \delta_s = \pi$<br>$\cos\gamma = 2\sin^2\gamma_n \cos^2\varepsilon_n - 1$ |
| $k_1 = k_2 = k_3$ | $k_1 \cos\gamma = \text{constant}$ | |

Each crystal shape, determined by the mutual relations between $A_i$ must be investigated for all possible combinations of relationship between $k_i$ and $A_i$ (see eq. (A.3)). This is done for three of them in table III. Obviously $k_1 = k_2 = k_3 = 0$ is impossible. All other combinations can also be omitted. They refer to orientations where a plane with a lower $A_i$ provides a contribution towards the vertical growth rate whereas a plane with a lower $A_i$ does not. Clearly lower maxima would be found than in the cases of table III.

TABLE III

| | | admitted combinations of relations between $k_i$ and $A_i$ | | |
|---|---|---|---|---|
| | | $k_1 = A_1$<br>$k_2 = A_2$<br>$k_3 = A_3$ | $k_1 = A_1$<br>$k_2 = A_2$<br>$k_3 = 0$ | $k_1 = A_1$<br>$k_2 = 0$<br>$k_3 = 0$ |
| possible crystal shapes | $A_1 > A_2 > A_3$ | $k_1 > k_2 > k_3$ | $k_1 > k_2 > k_3$ | $k_1 > k_2 = k_3$ |
| | $A_1 = A_2 > A_3$ | $k_1 = k_2 > k_3$ | $k_1 = k_2 > k_3$ | $k_1 > k_2 = k_3$ |
| | $A_1 > A_2 = A_3$ | $k_1 > k_2 = k_3$ | $k_1 > k_2 > k_3$ | $k_1 > k_2 = k_3$ |
| | $A_1 = A_2 = A_3$ | $k_1 = k_2 = k_3$ | $k_1 = k_2 > k_3$ | $k_1 > k_2 = k_3$ |

TABLE IV

| crystal shape | preferred orientations |
|---|---|
| $A_1 > A_2 > A_3$ | $\varepsilon_n = -\varepsilon_s$<br>$\delta_n + \delta_s = \pi$<br>$\cos\gamma = 2\sin^2\delta_n\cos^2\varepsilon_s - 1$ |
| $A_1 = A_2 > A_3$ | $\left.\begin{array}{l}\varepsilon_n = \varepsilon_s\\ \delta_n + \delta_s = \pi\\ \delta_n - \delta_s = \gamma\end{array}\right\}$ or $\left\{\begin{array}{l}\varepsilon_n = -\varepsilon_s\\ \delta_n + \delta_s = \pi\\ \cos\gamma = 2\sin^2\delta_n\cos^2\varepsilon_s - 1\end{array}\right.$ |
| $A_1 > A_2 = A_3$ | $\varepsilon_n = -\varepsilon_s$<br>$\delta_n + \delta_s = \pi$<br>$\cos\gamma = 2\sin^2\delta_n\cos^2\varepsilon_s - 1$ |
| $A_1 = A_2 = A_3$ | $\left.\begin{array}{l}\varepsilon_n = \varepsilon_s\\ \delta_n + \delta_s = \pi\\ \delta_n - \delta_s = \gamma\end{array}\right\}$ or $\left\{\begin{array}{l}\varepsilon_n = -\varepsilon_s\\ \delta_n + \delta_s = \pi\\ \cos\gamma = 2\sin^2\delta_n\cos^2\varepsilon_s - 1\end{array}\right.$ |

For these cases the relative maxima and the orientation at which they occur can be found in table II.

The highest maximum for all crystal shapes appears to be $\frac{1}{2}A_1(\cos\gamma + 1)$. The final results are tabulated in table IV and shown in fig. 8.

## Appendix B

*The calculation of the preferred orientation as a function of $\gamma$ in the special case of sec. 5.5*

The assumptions have been mentioned in sec. 5.5 and will not be repeated here.

Significance of hitherto not used symbols (dimension between brackets):

| | |
|---|---|
| $x$(m) | distance from surface $b$ (see fig. 14), |
| $B$(m) | width of surface $b$, |
| $D(\mathrm{m^2 s^{-1}})$ | diffusion coefficient of the fluid-like material of surface $a$, |
| $N(\mathrm{m^{-3}})$ | concentration of the solid and the fluid-like material, |
| $n_a, n_b(\mathrm{m^{-2}s^{-1}})$ | number of landing molecules on $a$ and $b$, respectively, |
| $A_a$, $A_b$ | acceptances of $a$ and $b$, respectively, |
| $m(\mathrm{m^{-2}})$ | number of fluid-like molecules per unit area, |
| $f(\mathrm{m^{-1}s^{-1}})$ | number of lateral-moving molecules per unit depth, |
| $V(\mathrm{m^{-2}s^{-1}})$ | total flux of molecular beam. |

The solidification rate on surface $a$ is $Kn$ in which $K(\mathrm{s^{-1}})$ is assumed to be a constant. The mass equation is

$$D\frac{\partial^2 m}{\partial x^2} = Km - n_a. \tag{B.1}$$

The boundary conditions are

$$m = n_a/K \quad \text{at} \quad x = \infty,$$
$$m = 0 \quad \text{at} \quad x = 0\ .$$

Solving the differential equation (B.1) gives

$$m = (n_a/K)\{1 - \exp\,[-x(K/D)^{1/2}]\}. \tag{B.2}$$

The total lateral transport across the crystal edge per unit depth can now be calculated:

$$f_{x=0} = n_a\,(D/K)^{1/2}.$$

The growth rate of plane $b$ is

$$\frac{n_a\,(D/K)^{1/2}}{NB} + \frac{n_b}{N}.$$

In the two-dimensional approach of fig. 14

$$n_a = V \sin(\gamma - \beta) A_a$$

and

$$n_b = V \cos(\gamma - \beta) A_b.$$

The total vertical growth rate appears to be proportional to

$$P \sin(\gamma - \beta) \cos\beta + \cos(\gamma - \beta) \cos\beta,$$

with (B.3)

$$P = \frac{A_a}{BA_b}\left(\frac{D}{K}\right)^{1/2}.$$

From eq. (B.2) we learn that $n = 0$ at $x = 0$, so that $B$ is a constant and so, therefore, is $P$.

The maximum of expression (B.3) is found if

$$P = \tan(\gamma - 2\beta).$$

The relation between $\gamma$ and $\beta$ for several values of $P$ is plotted in fig. 15.

**Acknowledgement**

The author is indebted to Mr W. P. J. Fontein for the calculations of appendix A. He would also like to thank, amongst others, Mr G. W. van Oosterhout for his critical remarks on the manuscript.

*Eindhoven, January 1967*

## REFERENCES


[1]) H. Mayer, Physik dünner Schichten, Wissenschaftliche Verlaggesellschaft M.B.H., Stuttgart, Vol. II, 1955.
[2]) D. M. Evans and H. Wilman, Acta cryst. **5**, 731-738, 1952.
[3]) E. Bauer, Trans. 9th Vac. Symp. Am. Vac. Soc. (Los Angeles 1962), MacMillan Comp., New York, 1962, pp. 35-44.
[4]) R. W. Clapp Jr, J. appl. Phys. **33**, 2539-2541, 1962.
[5]) K. L. Chopra, Appl. Phys. Letters **7**, 140-142, 1965.
[6]) M. Francombe, Phil. Mag. **10**, 989-1010, 1964.
[7]) L. S. Polatnik and A. I. Fedorenko, Soviet. Phys. solid State **7**, 653-656, 1965.
[8]) J. M. Nieuwenhuizen and H. B. Haanstra, Philips tech. Rev. **27**, 115-119, 1965/66.
[9]) H. M. Wiedenmann and H. Hoffmann, Z. angew. Phys. **18**, 502-506, 1965.
[10]) L. Reimer and K. Freking, Z. Phys. **184**, 119-129, 1965.
[11]) A. van der Drift, Philips Res. Repts **21**, 289-303, 1966.
[12]) I. Langmuir, Phys. Rev. **8**, 149-176, 1916.
[13]) D. W. Pashley, Adv. Phys. **14**, 327-410, 1965.
[14]) H. Poppa, J. Vacuum Science and Technology **2**, 42-48, 1965.
[15]) J. E. Johnson, Vacuum microbalance techniques, Plenum Press, New York, 1965, Vol. 4, pp. 81-98.
[16]) J. A. Bennett, M. A. Novice and I. M. Watt, Condensation and evaporation of solids, Gordon and Breach, New York and London, 1964, pp. 620-629.
[17]) E. Bauer, Single crystal films symposium, Publication Division Pergamon Press, Oxford etc., 1964, pp. 43-67.
[18]) D. Bernstein, Vakuum-Tech. **14**, 190-192, 1965.
[19]) E. Bauer, Z. Kristallogr. Kristallgeom. **107**, 72-98, 1956.
[20]) W. G. Burgers and C. J. Dippel, Physica, **1**, 549-560, 1934.
[21]) M. Volmer and G. Adhikari, Z. phys. Chem. **119**, 46, 1926.
[22]) J. van der Waterbeemd, Physics Letters **16**, 97-98, 1965; Philips Res. Repts **21**, 27-48, 1966.
[23]) G. Ehrlich, Structure and properties of thin films, Wiley, New York, 1959, p. 423.
[24]) C. Snoek and J. Kistemaker, Adv. Electronics Electron Phys. **21**, 67-99, 1965.
[25]) C. Brunnée, Z. Phys. **147**, 161-183, 1957.
[26]) C. H. Weysenfeld, Philips Res. Repts Suppl. **1967**, No. 2.
[27]) F. O. Goodman, J. Phys. Chem. Solids **23**, 1269-1290, 1962.
[28]) E. Bauer, Z. Kristallogr. Kristallgeom. **107**, 290-317, 1956.
[29]) M. Volmer, Kinetik der Phasenbildung, Steinkopf, Dresden-Leipzig, 1939, p. 56.